

## CuI.AgI AND CuI.ZnI<sub>2</sub> SOLUTIONS AS CATHODES IN MAGNESIUM BASED SEAWATER ACTIVATED BATTERIES

R RENUKA

Central Electrochemical Research Institute, Madras Unit, CSIR Madras Complex, Chennai 600 113. INDIA

[Received: 24 May 1999

Accepted: 20 April 2000]

**CuI.AgI and CuI.ZnI<sub>2</sub> solid solutions have been evaluated for their performance as cathodes in magnesium based seawater activated batteries. The effects of molecular composition of the material, sulphur addition and temperature variation are discussed in the light of the IR, EPR, magnetic and conductivity data.**

**Keywords:** Silver-copper iodide, silver-zinc iodide solid solutions, cathodes, seawater activated batteries, magnetoresistance, magnesium batteries.

### INTRODUCTION

Recent studies on seawater activated batteries have focused on improving the performance of CuI cathode with the objective of developing a cathode material that will be AgCl<sup>-</sup> equivalent in performance and at the same time cost effective [1]. The developmental work in this pursuit included investigation on CuI-containing additives such as AgCl and Ag<sub>2</sub>S [2], sulphur allotropes like S<sub>6</sub> and S<sub>12</sub> [3] and aromatic disulphide [4]. In the present work, the use of CuI.AgI and CuI.ZnI<sub>2</sub> solid solutions as cathodes in seawater activated cells is examined.

### EXPERIMENTAL

Unless otherwise specified all chemicals used were E Merck extra pure products. Double distilled water was used in preparing the solutions. CuI.AgI and CuI.ZnI<sub>2</sub> solid solutions of different molecular compositions were prepared by a coprecipitation technique following reported procedures [5-6].

The active material (equivalent to 0.36 Ah) was mounted on a thin copper mesh of dimension 0.04 m x 0.025 m x 0.02 m wrapped with filter paper and pressed using a hydraulic press. A compaction pressure of 10 tonnes was found to give a good performance. No binder was added [5].

The anode was made from magnesium alloy [AZ31] sheets of dimensions 0.04 m x 0.025 m x 0.015 m and the connection rivets fixed to the plates. The plates were first cleaned with acetone and then with concentrated HCl.

A cathode plate was placed between two magnesium anodes, a pair of thin PVC wires pasted on the inner side of magnesium plates/prevented direct contact of the cathodes with the anodes.

The cell was connected in series to a variable resistor and in parallel to a voltmeter and then immersed in a 100 ml beaker containing 3.3% NaCl as the electrolyte. All the discharges were constant current drains (100 mA) and were carried out at room temperature (298 ± 1 K). However, the internal resistance of the cell was measured as the slope of the plot of cell voltage against current density. A 250 W tungsten halogen lamp (130 mW.cm<sup>-2</sup>) with a transparent perspex cell was used for the experiments under white light.

For conductivity measurement, the end of discharge product was first washed thoroughly with water, dried at 353 K ground into a powder and then washed under a stream of water when the lighter colloidal graphite was washed away. It was dried at 353 K in an oven and made into a pellet of 0.06 m diameter and 0.002 m thickness. Electrical contact points were made with gold

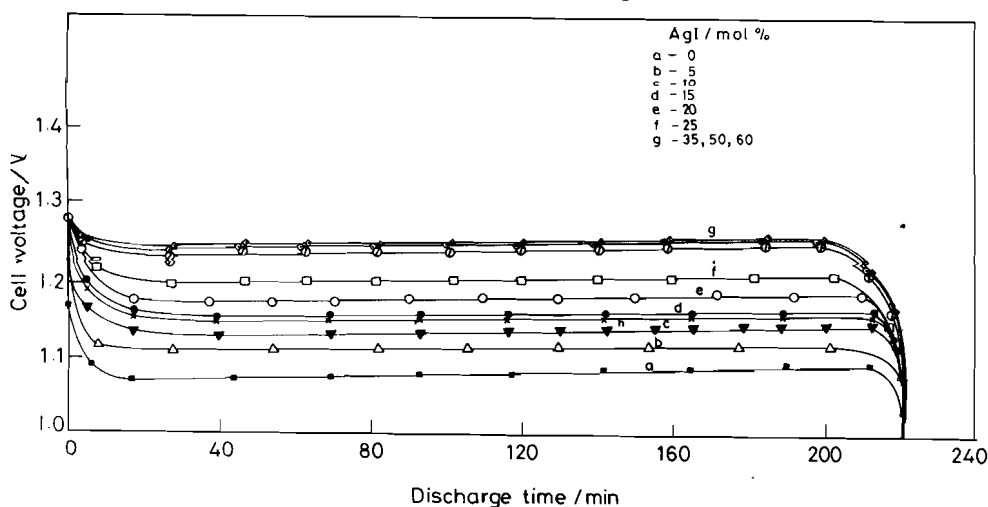


Fig. 1: Discharge curves of CuI.AgI solid solutions of different compositions. AgI (mol%) (a) 0 (b) 5 (c) 10 (d) 15 (e) 20 (f) 25 (g) 35,50, 60

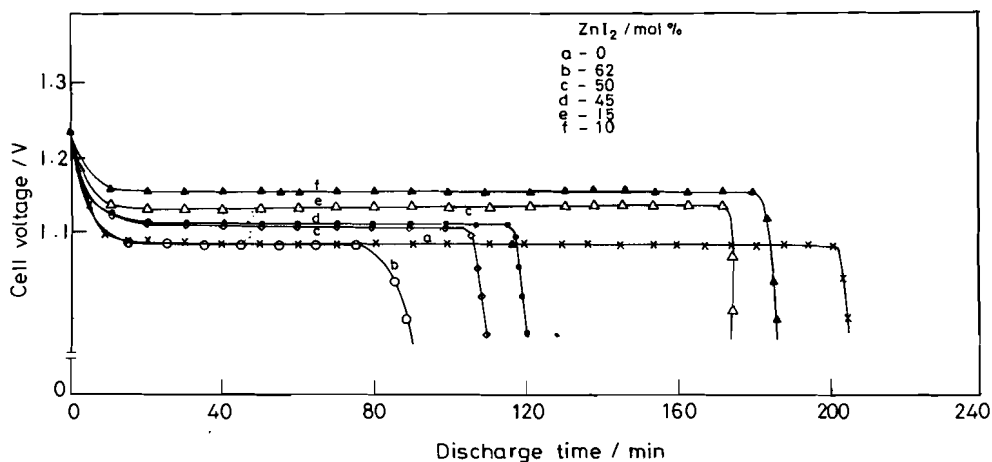


Fig. 2: Discharge curves of CuI.ZnI<sub>2</sub> solid solutions of different compositions. ZnI<sub>2</sub> (mol%) (a) 0 (b) 62 (c) 50 (d) 45 (e) 15 (f) 10

deposit/silver paint. Conductivity was measured using an assembled Hall and Vander Pauw system.

Diffuse reflectance electronic spectra were obtained with a Perkin Elmer Lambda - 9 double beam double monochromator UV/visible/infrared spectrophotometer using an integration system with BaSO<sub>4</sub> as the reference. A 250 W tungsten halogen lamp 130 mW.cm<sup>-2</sup> with a transparent perspex cell was used for the experiments under white light.

The magnetoresistance of the end of discharge product was measured on a Faraday dc magnetic susceptibility balance suitably home modified for measuring magnetoresistance. The balance was attached to a Keithley 224 programmable current source. Keithley 182 sensitive digital voltmeter and a Lake Share Cryotronics

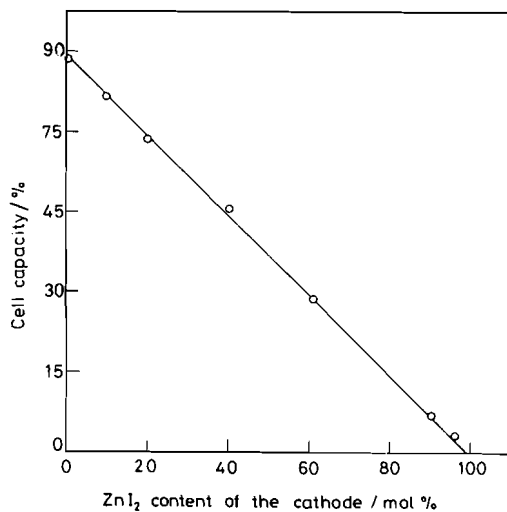


Fig. 3: Effect of ZnI<sub>2</sub> content on the capacity of the CuI.ZnI<sub>2</sub> cell

TABLE I: Cell voltage and internal resistance of S added (10 wt%) CuI.Agl-Mg seawater activated battery

Composition of the cathode		S/ wt%	Cell voltage/V	Cell resistance/ mΩ
*cg/ wt%	CuI.Agl/ mol% AgI			
10	0	0	1.08	25.13
10	10	0	1.13	18.94
10	20	0	1.18	17.83
10	30	0	1.22	16.71
10	35	0	1.24	15.60
6	30	0	1.20	16.44
6	30	5	1.42	13.38
10	30	10	1.65	11.97
10	30	12	1.70	12.49
10	30	15	1.63	13.69
10	0	10	1.36	20.98
10	30	20	1.40	17.19

\* colloidal graphite

temperature controller. The end of discharge product was cleaned by the same procedure as adopted for the conductivity measurement, it was then dried well. The sample thus prepared was sealed under vacuum and heated in a furnace to 1273 K for 24 h and left to cool in a horizontal position. Silver telluride and La<sub>0.75</sub>Ca<sub>0.25</sub>MnO<sub>3</sub> used for comparison purposes were gift samples from Prof B Viswanathan, Indian Institute of Technology, Chennai.

TABLE II: Cell voltage and internal resistance of S (10 wt%) added CuI.ZnI<sub>2</sub>-Mg seawater activated battery

ZnI <sub>2</sub> in the cathode mol%	Cell voltage/V	Cell resistance/ mΩ
0.0	1.36	20.38
5.0	1.38	18.01
7.5	1.40	13.39
10.0	1.42	10.84
20.0	1.35	11.93
30.0	1.30	12.73
35.0	1.27	13.66
40.0	1.26	14.78
50.0	1.25	15.33
60.0	1.15	17.32
70.0	1.14	22.99
80.0	1.14	23.28
90.0	1.12	22.74

The electrochemical measurements were performed in a microcell at 298 K with the use of a conventional three electrode configuration consisting of a highly polished glassy carbon working electrode (area 0.28 cm<sup>2</sup>) from BAS Ltd, a platinum-wire auxiliary electrode and an Ag/AgCl reference electrode containing 3 mol.dm<sup>-3</sup> NaCl solution. Spectral grade acetonitrile was used with out further purification. The supporting electrolyte (NBu<sub>4</sub>PF<sub>6</sub>) (Fluka Chemie AG Industries) was recrystallised twice from ethanol and water and dried under vacuum in a oven at 353 K for 12 h. The cell compartment was filled with solvent- saturated nitrogen to

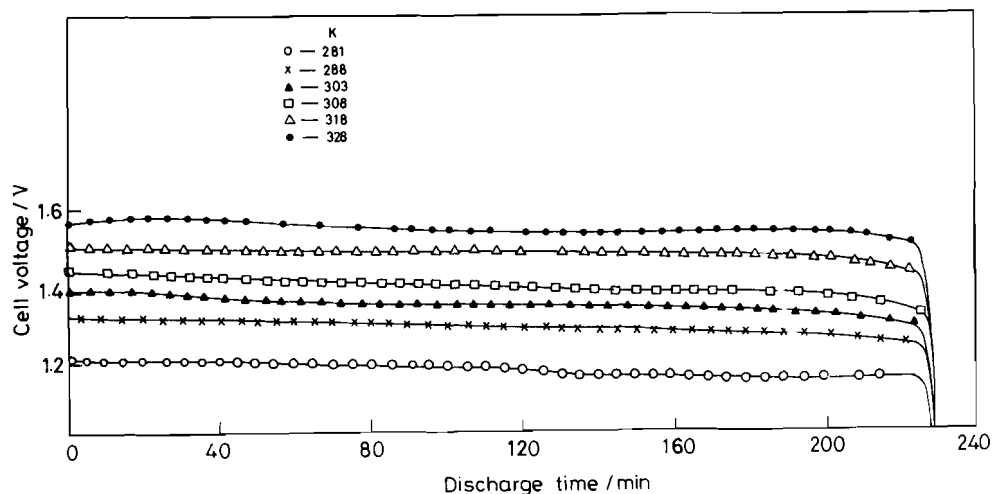


Fig. 4: Effect of temperature on the discharge performance of Mg-CuI.Agl (70 mol% CuI) cell

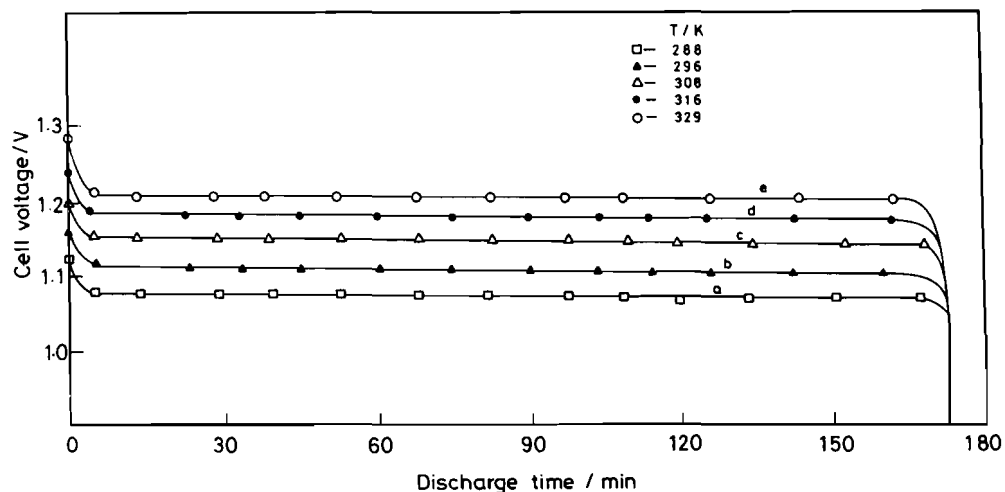


Fig. 5: Effect of temperature on the discharge performance of Mg-CuI.ZnI<sub>2</sub> (80 mol% ZnI<sub>2</sub>) cell

deerate the solution. Ferrocene was used as an internal standard. Potentials for the compound are reported vs corrected Ag/AgCl. The half-wave potential of the ferrocene ferrocenium couple under the conditions employed was 0.45 V (E = 60 mV) vs Ag/AgCl.

### RESULTS AND DISCUSSION

#### Effect of molecular composition of the cathode and temperature on battery performance

The discharge curves of CuI.Agl and CuI.ZnI<sub>2</sub> of different compositions are presented in Figs. 1 and 2 respectively. The cell voltage is dependent on the molecular composition reaching a maximum at 40 mol% CuI in the case of CuI.Agl and at ≥ 80 mol% CuI in the case of

CuI.ZnI<sub>2</sub>. It is reasonable to associate this feature to the fact that compositions with > 10 mol% AgI are solid solutions [2] and > 40 mol% CuI in CuI.Agl and CuI.ZnI<sub>2</sub>, respectively, are solid solutions [7-8]. The ZnI<sub>2</sub> portion of CuI.ZnI<sub>2</sub> does not seem to contribute to the cell capacity because the observed capacity is proportional to the CuI content of the cathode only. In other words, as ZnI<sub>2</sub> content increased, the cell capacity decreased (Fig. 3).

Internal resistance of the cell was measured as the slope of the plot of cell voltage against current density and the values are listed in Tables I and II. The cell voltage is dependent on the internal resistance of the cell. In the range 10-60 mol% AgI in the CuI.Agl cathode and

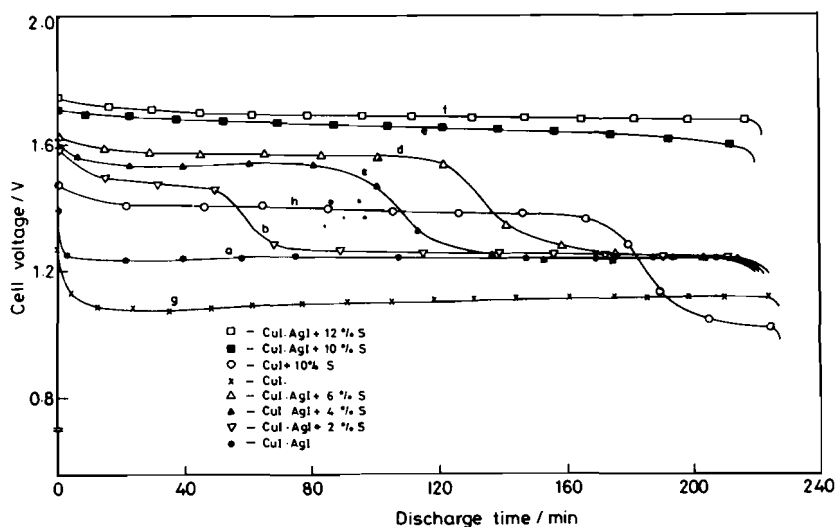


Fig. 6: Discharge curves of CuI.Agl solid solutions (70 mol% CuI) in the presence of sulphur

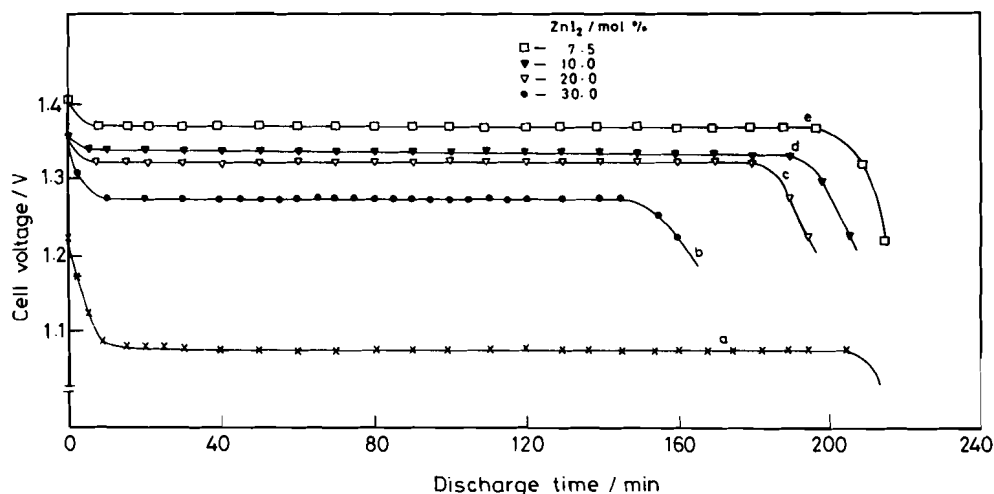


Fig. 7: Discharge curves of 10 wt% S added CuI.ZnI<sub>2</sub> (60 mol% ZnI<sub>2</sub>)

10-50% ZnI<sub>2</sub> in the CuI.ZnI<sub>2</sub> cathode, there is significant decrease in the internal resistance of the cell as compared with that of the cell containing CuI.

The discharge curves of the Mg-CuI.AgI cell of 70 mol% CuI and Mg-CuI.ZnI<sub>2</sub> cell of 80 mol% CuI compositions at various temperatures are shown in Figs. 4 and 5 respectively. There is a gradual increase in the cell voltage with temperature, although there is not much change in the delivered capacity.

#### Effect of sulphur addition

It is common practice to add sulphur to the cathode active material in Mg-copper compound water activated batteries in order to enhance the cell voltage [7-13]. Besides increasing the cell voltage sulphur is also reported to promote the utilisation efficiency of the cathode active material. The present study investigated the effect on the

battery performance of adding S to the cathode. The discharge curves of CuI.AgI of >70 mol% CuI composition in presence of S are shown in Fig. 6. The discharge curves of 10 wt% S added CuI.ZnI<sub>2</sub> of composition 60 mol% CuI are shown in Fig. 7. It is observed that sulphur addition brings about a remarkable increase in cell voltage both of the Mg-CuI.AgI and Mg-CuI.ZnI<sub>2</sub> batteries and the increase is higher than the increase of cell voltage effected by sulphur addition to CuI in Mg-CuI cells. But the sulphur benevolence depends on the molecular composition of the cathode. At a sulphur content of 10 wt% in the CuI.AgI cathode, an increase in the AgI content over CuI results in a decrease in conductivity of the end of discharge product. This effect is due to the absence of appreciable voltage-elevating effect of sulphur on silver halide cathodes as verified by the discharge performance studies of S-laden

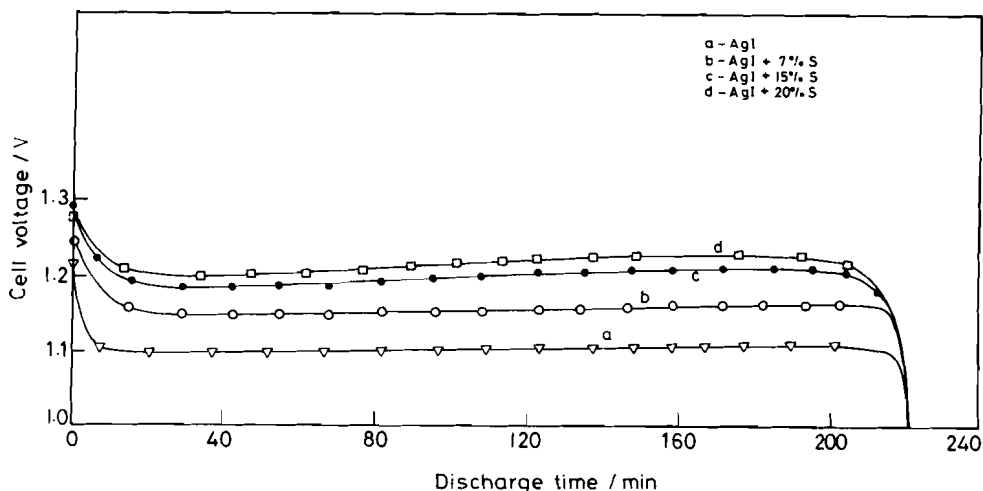


Fig. 8: Discharge performance of S added AgI cathode

**TABLE III: Conductivity of end of discharge products of sulphur containing CuI.AgI cathode**

Composition of the cathode mix		
AgI/mol%	S/wt%	Conductivity/S cm <sup>-1</sup>
0	—	3.14 × 10 <sup>-7</sup>
0	10	4.82 × 10 <sup>-4</sup>
10	0	4.33 × 10 <sup>-4</sup>
10	5	5.09 × 10 <sup>-4</sup>
10	10	5.88 × 10 <sup>-4</sup>
10	—	6.14 × 10 <sup>-4</sup>
20	15	6.44 × 10 <sup>-4</sup>
20	15	6.48 × 10 <sup>-4</sup>

AgI (Fig. 8). A point of interest with S addition to CuI.AgI is that the compacted electrode was very shiny and had a metallic appearance. The author observed a similar feature with Ag<sub>2</sub>S added to CuI cathode. CuI.AgI is malleable and ductile which may be expected to confer the above qualities to the cathode mix. Another important observation made in this case is that 6% of colloidal graphite was adequate to match the performance of a 10% colloidal graphite containing CuI cathode (Table 1).

In the case of S-laden CuI.ZnI<sub>2</sub>, the assistance provided by zinc was verified by studying the effect of light incidence on cathode during discharge. There was a slight increase in cell voltage and capacity of the battery upon light incidence. This improved efficiency is due to the photoconductive nature of ZnS [14]. The extent of chemical reaction in battery depends among other things on the electrical conductivity of the intermediate layer formed at the electrode surface. It has been shown that, introduction of S, an electron acceptor into Cu<sub>2</sub>O or CuCl [12] or CuI [1] could result in a manifold increase in the conductivity of the intermediate which is depleted during discharge. A previous work [3] on Mg-CuI seawater activated battery indicated the possibility of formation of mixed valent Cu<sup>+</sup>-Cu<sup>2+</sup> sulphide and/or complex sulphides and/or copper polysulphides in the discharge of S containing CuI cathode. Similarly in the study of the effect of AgCl and Ag<sub>2</sub>S on CuI, the formation of copper-silver iodide sulphide was proposed [2]. The present observation of a higher voltage elevating effect of S both on CuI.AgI and CuI.ZnI<sub>2</sub> over that of CuI is a clear indication of the assistance provided by coexistent silver and zinc, respectively. The cell voltage is dependent

on the internal resistance of the cell. In the range 10-60 mol% AgI in the CuI.AgI cathode and 10-50% ZnI<sub>2</sub> in the CuI.ZnI<sub>2</sub>, there is a significant decrease in the internal resistance of the cell as compared with that of the cell containing CuI (Tables I and II). However, in the presence of excess sulphur, some irregularity in the variation of internal resistance is noticed. Further, above 60 mol% AgI, there is an increase in the cell resistance (Tables I and II).

#### Composition dependence on dc conductivity

The conductivity data of the end of discharge products of S-added CuI.AgI are presented in Table III. The conductivity values are higher than those of the end of discharge products of S-containing CuI.

One observes a remarkable change in conductivity with AgI content. From their calorimetric studies on silver based glasses, it has been [15] proposed a model structure for glass called the mixed electrolyte tissues to amorphous AgI aggregate. AgI aggregates are proposed to exist in the mixed electrolyte tissue model. The model has some kind of amorphous structure which depends on the size of the AgI aggregate region which is expected to grow in size with AgI composition. They suggested that the fast ion conduction in silver based glasses seems to originate from the presence of positional disorder of mobile Ag<sup>+</sup> ions. The number of such mobile Ag<sup>+</sup> ions (and which dominate the conduction) increases with AgI aggregates concentration. The above model appears to suit CuI.AgI solid solutions also.

The CuI network and the presence of I<sup>-</sup> ions reduce the activation barrier for the silver ions since the interaction

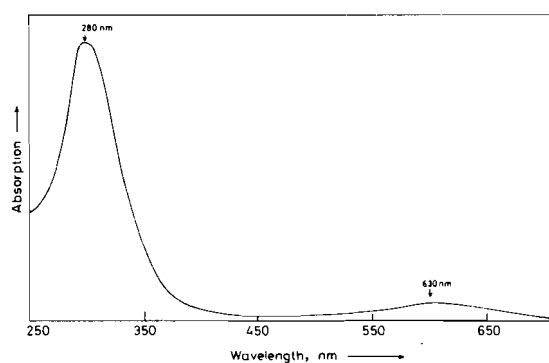


Fig. 9: Diffuse reflectance spectrum of the end of discharge product of 10 wt% S added CuI.AgI (90 mol% CuI)

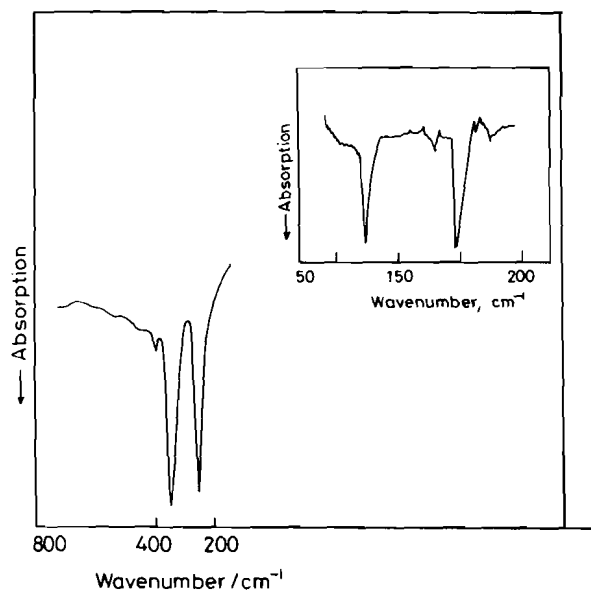


Fig. 10 IR spectrum of the end of discharge product of 10 wt% added CuI.Agl (90 mol% CuI). Inset: Far IR spectrum of the end of discharge product of 10 wt% S added CuI.Agl (90 mol% CuI)

of these ions with Ag<sup>+</sup> forms a shallow potential well with a reduced barrier. The size of the AgI aggregates and also the number of Ag<sup>+</sup> ions surrounding the I<sup>-</sup> ions increase with AgI concentration and hence the number of Ag<sup>+</sup> ions located in the shallow potential well increases. When the shallow potential wells are connected for a long time, they form an easy path favourable for the transport of Ag<sup>+</sup> ions. However, there is a decrease in conductivity above 60 mol% AgI in the cathode material. This observation could be explained on the basis of formation of a glassy polycrystalline mixture at such high AgI concentrations [16].

#### Analysis is end of discharge products

By chemical and XRD analysis, the end of discharge product of the CuI.Agl and CuI.ZnI<sub>2</sub> solid solutions were characterised to be respective alloys of the two metals occurring in quantities proportional to the molecular composition of the starting material of the cathode. Since the introduction of the ZnI<sub>2</sub> component hampers the capacity of the battery and sulphur addition is not very beneficial to the CuI.ZnI<sub>2</sub> cells, the analysis of end of discharge product was restricted to CuI.Agl cathodes only. In the case of sulphur addition (10 wt%) the end of discharge product was blackish brown in colour and a

qualitative inorganic analysis of the product confirmed it to be a sulphide. A chloroform extract of the product did not show the characteristic UV spectrum of sulphur ( $\lambda_{\text{max}} = 290 \text{ nm}$  [17]) indicating absence of free sulphur in the end of discharge product.

#### UV-Vis and IR spectra

The solid state diffuse reflectance spectrum of the compound (Fig. 9) showed an intense band at 280 nm with a tail at 630 nm. Ag<sup>+</sup> in 2 or 3 coordinate environments of sulphur containing ligands are known to absorb in this region [18-22].

IR data (Fig. 10) obtained for the end of discharge at 384 cm<sup>-1</sup> are confirmation of the existence of metal-sulphur bonding. In addition, the spectrum also presents absorption peak at 174 cm<sup>-1</sup> which can be associated with metal-halide bonding particularly a bridging halogen bonding [23]. This orientation indicates the presence of I<sup>-</sup> in the end of discharge product. The same was confirmed by a positive result in the test for iodide. The far IR absorption (Fig. 10 inset) confirms metal-metal bonding [24]. In general,  $\nu_{(\text{MM})}$  appear in the low frequency region (250- 100 cm<sup>-1</sup>) because the M-M

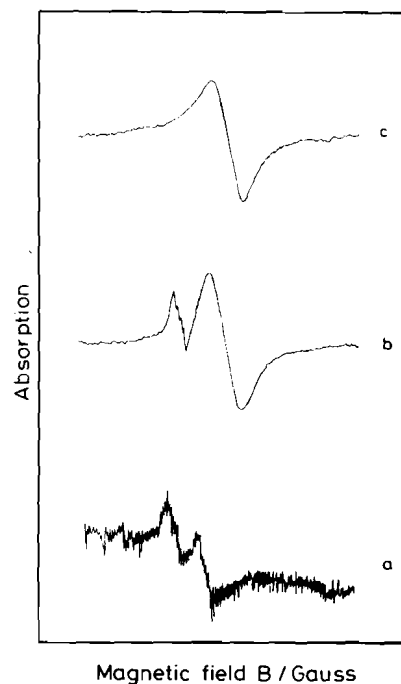


Fig. 11: EPR spectrum of the end of discharge product of (a) 10 wt% S added CuI; (b) 10 wt% S added CuI.Agl (30 mol% CuI); (c) 10 wt% S added CuI.Agl (90 mol% CuI)

bonds are relatively weak and the masses of metals are relatively large.  $\nu_{(M-M)}$  vibrations of a heteronuclear complex is expected to be stronger because of the presence of a dipole moment along the metal-metal bonds. The strong absorption of the end of discharge product at  $110\text{ cm}^{-1}$  provides an indication that the end of discharge product is a copper-silver sulphide iodide.

**EPR spectra and magnetic measurements**

The EPR spectra (Fig. 11) of the end of discharge product in the case of sulphur-added CuI.Agl present some interesting features. At higher concentrations of AgI in the starting material of the cathode the spectral pattern (Fig. 11) is somewhat similar to that (Fig. 10) of the end of discharge product of S-added CuI. At higher CuI concentrations, the EPR spectrum consists of a single quasi-symmetrical signal with no hyperfine splitting which allows the calculation of g at 2.07. The low value obtained for g can be attributed to intermolecular spin coupling interactions.

Magnetic measurements made on the product show a strong temperature dependence of magnetic dropping from a value of 1.35 BM at 300 K to 0.69 BM at 5 K. The plot of inverse susceptibility versus temperature shows two distinct linear dependence ranges. The effective magnetic moment from the RT product for each showed a monotonic decrease is observed from room temperature to 2 K. This behaviour can only be explained by supposing that intermolecular interactions become important as the temperature is lowered.

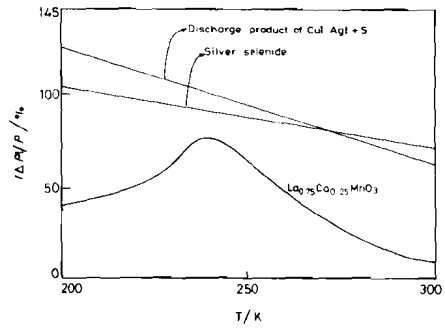


Fig. 13: Magnetoresistance of the end of discharge product of 10 wt% S added CuI.Agl (60 mol% CuI)

In fact the magnetic susceptibility measurements was sought as a quicker method to confirm the existence of diamagnetic Cu<sup>+</sup> in the sulphide (i.e. end of discharge product). But paramagnetic behaviour has been outlined in previous paragraphs. It is thus evident that the sulphide formed does not consist exclusively of Cu<sup>+</sup> ions and the presence of Cu<sup>2+</sup> ions is indicated. In an earlier work [3], the possibility of formation of cuprous- cupric mixed valent sulphide in the discharge of CuI cathode was shown. The same proposition seems to hold good in the present context also. Supportive evidence for the existence of Cu<sup>2+</sup> is provided by the proof that in CuI.Agl solid solutions, Cu<sup>2+</sup> and Ag<sup>+</sup> ions co-exist at high CuI concentrations, whereas at high AgI concentrations, the presence of Cu<sup>2+</sup> is rendered difficult by silver occupying the interstitial sites [25]. The dependence of the EPR spectral battery of the discharged product on the CuI.Agl

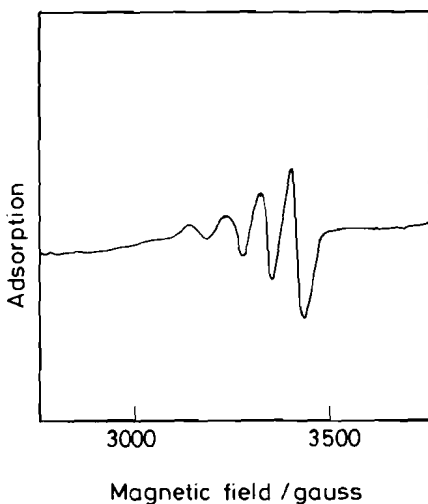


Fig. 12: EPR spectrum of the end of discharge product of 10 wt% S added CuI.Agl (30 mol% CuI). Medium: CH<sub>3</sub>CN

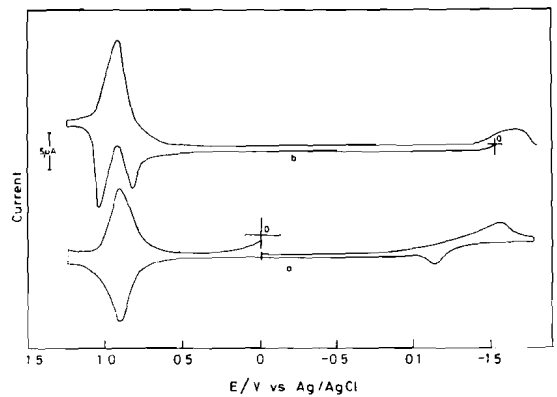


Fig. 14: Cyclic voltammogram of (a) CuI.Agl (90 mol% CuI) (b) end of discharge product 10 wt% S added. CuI.Agl (90 mol% CuI)

ratio of the cathode material is in agreement with this concept. This proposition was further supported by the solution (CH<sub>3</sub>CN medium) EPR spectrum (Fig. 12) of the product which showed four lines characteristic of the presence of Cu<sup>2+</sup> ions. Put together, these observations suggest that the end of discharge product of 10 wt% S-added 90:10 CuI.Agl should be considered as a Cu<sup>+</sup>-Cu<sup>2+</sup> mixed valent compound with a single unpaired electron per Cu<sup>2+</sup> unit.

### Magneto-resistance measurement

It has been [26] recently reported large magneto-resistance in silver selenides and silver tellurides. This revolutionary discovery introduces a hitherto unexplored class of magneto-resistive compounds, the silver chalcogenides which are by nature non-magnetic. Ag<sub>2</sub>S, Ag<sub>2</sub>Se and Ag<sub>2</sub>Te are superionic conductors; below 400 K, ion migration is effectively frozen and the compounds are non-magnetic semiconductors [27] that exhibit no appreciable magneto-resistance [28]. It has been [26] showed that slightly altering the stoichiometry can lead to a marked increase in the magnetic response.

This finding of a large magneto-resistance in silver chalcogenides provided the enthusiasm to make an attempt on the measurement of magneto-resistance of the end of discharge product in the case of 10 wt% S added 60 mol% CuI 40 mol% AgI cathode. The results are presented in Fig. 13. It is interesting to note that the product shows a response similar to that of silver selenide with an unusual linear dependence on magnetic field.

The present observation adds a new perspective to the study of magneto-resistance of silver chalcogenides. By now we have identified that the end of discharge product of the S added CuI.Agl is a sulphide iodide that consists of mixed valent copper ions (i.e. Cu<sup>+</sup>-Cu<sup>2+</sup> and Ag<sup>+</sup> ions. Although the exact stoichiometry of the iodide sulphide has not yet been arrived at the material marks the beginning of discovery of a series of novel chalcogenides that exhibit appreciable magneto-resistance. It is to be noted that the study as described in [26] is restricted to silver selenides and tellurides. The behaviour of silver sulphides may be similar to or different from that of the heavier chalcogenides and remains to be analysed. In the present context of chalcogenide physics, it is worth mentioning about discovery of superconductivity in compressed sulphur. It has been described [29] who have made this discovery report that given the comparative

simplicity of elemental sulphur for electronic structure, calculation and knowledge of its high pressure crystal structure, this element should provide important tests of possible new mechanisms for superconductivity. The findings have been reported [26-29] almost at the same time (Nov 1997). The two independent works put together present a promising growth for study in silver sulphides. Further there would be a tremendous impact of such findings on the development of novel seawater activated batteries. Such a proposition is further strengthened by the fact that sulphur allotropes like S and S bring about an elevation in cell voltage of Mg-CuI cells, the elevation being much above that produced by the commercial orthorhombic sulphur variety [3]. A point of relevance to the present discussion is that certain electrolytes for all solid state batteries could be candidates for cathodes in seawater activated batteries.

### Cyclic voltammetry

Fig. 14 shows a typical cyclic voltammogram of 90:10 CuI.Agl in CH<sub>3</sub>CN medium Cu<sup>+</sup>/Cu<sup>2+</sup> oxidation is observed at E<sub>p</sub>, a = +0.90 V with the corresponding reverse peak at E<sub>p</sub>, c = +0.96 V. The Ag<sup>+</sup> reduction wave appears at -0.11 V. The reoxidation of the Ag<sup>0</sup>/Ag<sup>+</sup> couple occurs at -0.165 V. The cyclic voltammogram of the end of discharge product of 10 wt% S-laden 90:10 CuI.Agl shows absence of Ag<sup>+</sup> reduction wave in the first cycle, whereas the Cu<sup>+</sup>/Cu<sup>2+</sup> oxidation is persistent with a slight increase in the peak current. The negative going sweep shows two waves typical of two electron transfer (at different E<sup>0</sup> values) to a Cu<sup>+</sup>/Cu<sup>2+</sup> species [30-32].

### CONCLUSION

CuI.Agl and CuI.ZnI<sub>2</sub> solid solutions of different molecular compositions have been examined as cathodes in magnesium based seawater activated batteries. The following conclusions have been drawn.

- The cell voltage of the Mg-CuI.Agl and Mg-CuI.ZnI<sub>2</sub> cells is dependent on the composition of the cathode. In the case of CuI.Agl, the cell voltage increase with AgI content upto 60 mol% beyond which there is not appreciable change. In the case of CuI.ZnI<sub>2</sub> there is some increase in the cell voltage with increase ZnI<sub>2</sub> content. However, beyond 20 mol% the cell voltage drops. Further, the ZnI<sub>2</sub> component does not seem to contribute to cell discharge capacity.

- The voltage-elevating effect of sulphur on the cathode, operates over a small range of cathode composition, viz., ≤ 10 mol% AgI and ≤ 30 mol% ZnI<sub>2</sub>. At concentrations higher than this range, sulphur addition is not beneficial to cell performance.
- The cell voltage increases with temperatures in the range of 288-338 K, although there is not a marked variation in the delivered capacity.
- EPR spectral measurements support the presence of mixed valent copper (Cu<sup>+</sup>-Cu<sup>2+</sup>) in the end of discharge product of the S added CuI.Agl.
- The end of discharge product of S containing CuI.Agl exhibits appreciable magnetoresistance.

Reported evidence shows that several major magneto-structural correlations have arisen out of the studies on Cu(II) halide layer perovskites [33-36] and such materials are of importance in low dimensional magnetism [37]. The observation made in the present study and arising out of battery performance evaluation indicates great scope for further studies that aim at battery as a tool to tap energy and at the same time for synthesizing novel compounds of practical importance. It is hoped that there would be intense activity in such trans-disciplinary areas of investigation.

**Acknowledgment:** The author is grateful to Prof B Viswanathan, IIT Madras, Chennai for facilities and helpful discussions.

## REFERENCES

1. J P Muller and P L Howard, *Trans Electrochem Soc*, **90** (1946) 529
2. R Renuka, *J Appl Electrochem*, **27** (1997) 1394
3. R Renuka, *Mater Chem Phys*, **59** (1999) 42
4. R Renuka, *J Appl Electrochem*, **29** (1999) 271
5. B Ray and P Septon, *Phys Status Solids*, **88** (1985) 261
6. A M Grayson and R Brian, *Mater Res Bull*, **12** (1984) 1527
7. Y Aoki and M Hiroi, *Bull Electrochem Soc Jpn*, **67** (1968) 169
8. N Margalit, *J Electrochem Soc*, **122** (1975) 1005
9. M Hiroi, *J Appl Electrochem*, **16** (1986) 431
10. R F Koontz and L E Klein, *U S Patent*, **419** (1990) 2913
11. R F Koontz, *U S Patent*, **4007316** (1977)
12. M Hiroi, *J Appl Electrochem*, **15** (1985) 201
13. V Flerov, *Zh Prikl Khim*, **34** (1961) 1929
14. W W Piper, *Phys Rev*, **98** (1955) 1015
15. M Nakayama, M Hanaya, A Hatate and M Oguni, *J Noncryst Solids*, **172** (1994) 1252
16. N Baskaran, G Govindaraj and A Narayanasamy, *Solid State Ionics*, **98** (1997) 217
17. H P Koch, *J Chem Soc*, (1949) 394
18. J G Wright, M J Natan, F M Mac Donnell, D M Ralston and T V O'Halloran, *Prog Inorg Chem*, **38** (1990) 323
19. G A Bowmaker in, "Spectroscopy of Inorganic Based Materials" (Eds) R J H Clerk and R E Hester, John Wiley & Sons, New York (1987) 1-117
20. A L Rheinyold, S Munavalli, D I Rossman and C P Ferguson, *Inorg Chem*, **33** (1994) 1723
21. J G Dance, *Aust J Chem*, **31** (1978) 2155
22. E Block, M German, H Kang, G Ofori-Okai and G Zubieta, *Inorg Chem*, **28** (1989) 1263
23. K Nakamoto, "Infrared and Raman Spectra of Inorganic and Coordination Compounds, 3rd edition, Wiley Interscience, Chichester (1978) 325
24. E Block, M German, H Kang, G Ofori-Okai and G Zubieta, *Inorg Chem*, **28** (1989) 322
25. B Ray, J Brightwell and P Stephen, *J Lumin*, **37** (1987) 133
26. R Xu, A Husmann, T F Rosenbaum, M L Saboungi, J E Enderby and P B Littlewood, *Nature*, **390** (1997) 57
27. R Dalven and R Gill, *Phys Rev*, **159** (1967) 645
28. P Junod and Helv, *Phys Acta*, **32** (1959) 567
29. V V Struzhkin, R J Hemley, J K Ma and Y A Timofel'v, *Nature*, **390** (1997) 382
30. G S Long, M Wer and R D Willett, *Inorg Chem*, **36** (1997) 3102
31. M Middle Ton, H Place and R D Willett, *J Amer Chem Soc*, **110** (1998) 8039
32. B J Hathaway, in Sir G Wilkinson (Ed), "Comprehensive Coordination Chemistry - The synthesis, reactions, properties and applications of coordination compounds", Pergamon, Oxford, **5** (1987) 533
33. C P Lander, K Harvorson and R D Willett, *J Appl Phys*, **61** (1987) 3255
34. C Chow, K Chang and R D Willett, *J Chem Phys*, **59** (1973) 2629
35. L J De Jongh and A R Miedema, *Adv Phys*, **23** (1974) 1
36. P M Richards and M B Salamon, *Phys Rev B*, **9** (1974) 32
37. T M Kite and J E Drumbeller, *J Mag Reson*, **54** (1983) 253